Biomaterials Science

RSC Publishing

COMMUNICATION

Controlled adhesion and proliferation of a human osteoblastic cell line by tuning the nanoporosity of titania and silica coatings†

Cite this: *Biomater. Sci.*, 2013, **1**, 186

Received 26th July 2012,
Accepted 23rd October 2012

DOI: 10.1039/c2bm00136e

www.rsc.org/biomaterialsscience

Martín G. Bellino,[a] Sebastian Golbert,[a] Mauricio C. De Marzi,[b,c] Galo J. A. A. Soler-Illia*[a] and Martín F. Desimone*[d]

The engineering of surfaces to control cell adhesion represents an active area of biomaterials research. Herein, we demonstrate that it is possible to tune the adhesion and proliferation of a human osteoblastic cell line (Saos-2) by tailoring the nanopore size of an oxide film coating.

Cell–biomaterial interactions are largely governed by the stiffness and chemical composition of the substrate, although the surface topography has also been shown to play an important role in the adhesion and proliferation of various cell types to different substrates.[1] At present, the engineering of surfaces to control cell adhesion represents an active area of biomaterials research that aims to meet the requirements of each cell–biomaterial interaction.[2–4] Particularly, improving the initial attachment of cells to implant surfaces may lead to an enhanced integration of the implant and longer term stability.[5,6]

Various techniques have been reported for creating substrates with a controlled topography on different materials. These include electron beam lithography and photolithography, which are two standard techniques for creating ordered features.[7] Whereas, polymer demixing, phase separation, colloidal lithography and chemical etching are most typically used for creating non-ordered surface patterns.[8] In this context, several studies report the interaction of various cell types with different micrometer and submicrometer topographies. However, the effect of nanotopographies has gained attention in recent years.[7,9] Nowadays it is possible to design substrates with different chemical, wettability and/or porosity properties that are routinely prepared by combining soft chemistry, supramolecular templates and surface modifications.[10–12] Particularly, evaporation induced self-assembly (EISA) is a versatile route towards thin films with a tunable mesoscopic topography that can open up new possibilities in advanced coatings for the control of cell behaviour.

In this work, we prepare mesoporous thin films with a tuned mesoporosity by the EISA method, which influences, and eventually leads to the control of, the adhesion and proliferation of Saos-2 cells to silica and titania substrates. This work contributes to the understanding of the influence of nanotopography on cell behaviour and the feasibility of applying the EISA method to tune the adhesion and proliferation of cells.

Titania and silica mesoporous thin films were prepared by dip-coating on glass substrates at a RH of 40–50%;[13,14] detailed procedures are described in the ESI.† Standard microscope glass slides used as substrates were cleaned with HNO_3 solution (5%), water and, finally, with ethanol. The dip-coating speed was 1 mm s^{-1}. $Si(OEt)_4$ (TEOS) and $TiCl_4$ were used as the inorganic precursors. Several surfactant templates were used: CTAB ($C_{16}H_{33}$–$N(CH_3)_3Br$), Brij-58 ($C_{16}H_{33}(OCH_2CH_2)_{20}$–OH), and Pluronics-F127 ($HO(CH_2CH_2O)_{106}(CH_2CH(CH_3)O)_{70}$-$(CH_2CH_2O)_{106}OH$). After deposition, the films were placed in 50% RH chambers for 24 h and subjected to a stabilizing thermal treatment procedure consisting of two successive 24 h heat treatments at 60 and 130 °C. Finally, films were calcined in air at 350 °C for 2 h with a 1 °C min^{-1} temperature ramp. Non-mesoporous SiO_2 and TiO_2 films (hereafter NMSi and NMTi samples respectively) were synthesized using the same solution compositions and thermal treatments as mesoporous films but without the surfactant template.

Water adsorption–desorption isotherms were determined by environmental ellipsometric porosimetry (EEP) according to current protocols.[15]

To test cell adhesion on the different materials, we added 1×10^3 Saos-2 cells to the surface of each type of coated glass.

[a]*Gerencia Química, Comisión Nacional de Energía Atómica, San Martín, Argentina. E-mail: gsoler@cnea.gov.ar*
[b]*Cátedra de Inmunologia, IDEHU-CONICET, Facultad de Farmacia y Bioquímica, Universidad de Buenos Aires, Junin 956, Piso 4° (1113), Buenos Aires, Argentina*
[c]*Departamento de Ciencias Básicas, Universidad Nacional de Lujan, Argentina*
[d]*IQUIMEFA-CONICET. Facultad de Farmacia y Bioquímica, Universidad de Buenos Aires, Junin 956, Piso 3° (1113), Buenos Aires, Argentina.*
E-mail: desimone@ffyb.uba.ar

†Electronic supplementary information (ESI) available: Detailed experimental procedures, film characterization, fluorescent microscope images of DAPI stained adhered cells at various times and statistical analysis. See DOI: 10.1039/c2bm00136e

The count of the total remaining DAPI stained adhered cells was performed with a fluorescent microscope (Olympus). The proliferation of adherent cells was determined by the tetrazolium assay.[16]

The EISA method leads to a set of uniform and smooth titania and silica thin films with tailorable mesoporous structures. Transparent and crack-free films were deposited by dip-coating a supramolecularly templated partially hydrolyzed oxide precursor. The use of CTAB, Brij-58 and Pluronics F127 surfactants allows different lyotropic mesophases to be obtained, thus creating surfaces with different pore sizes and symmetry after template removal.[11,12]

Typical H_2O-adsorption isotherms and pore size distributions of mesoporous films measured by EEP are shown in Fig. 1. A large pore volume and controlled pore dimensions (estimated from the adsorption branch) were obtained. In the case of F127-templated films with a cubic *Im3m* mesostructure, an average pore diameter of *ca.* 10 nm was observed (hereafter MSi-9 and MTi-10 samples for SiO_2 and TiO_2 mesoporous oxides, respectively). Smaller pore diameters were obtained in the case of Brij 58 (*Im3m*, 6 nm) and CTAB (3D hexagonal, $p6_3/mmc$, 4 nm),[10] hereafter MSi-4 and MTi-6 samples for SiO_2 and TiO_2 mesoporous oxides respectively. Pore dimensions obtained by EEP were in excellent agreement with electronic microscopy. Insets in Fig. 1 show typical TEM micrographs that illustrate the variety of mesoporous structures obtained, where the mesostructure and uniform pore size can be clearly observed in all cases.

Table 1 summarizes the mesoporous structural features and the surface energy obtained from water contact angle measurements (CA). Non-templated films are more hydrophobic than mesoporous ones; however, in the pore range explored, a higher contact angle is observed for films with a larger pore size. This complex behaviour can be attributed to the interplay of different texture and surface features.[17]

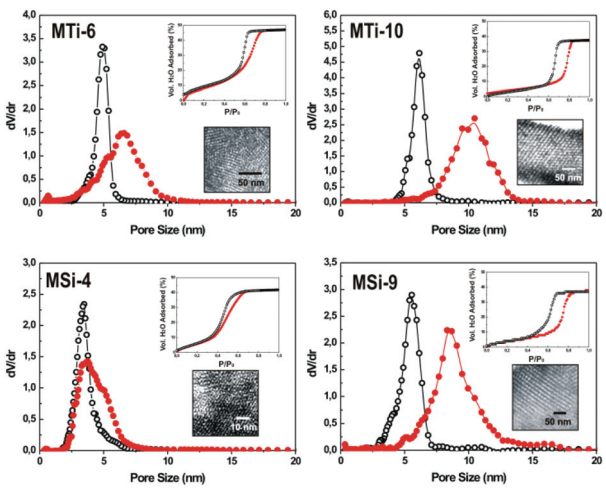

Fig. 1 Pore size distribution (red line) and neck size distribution (black line) of typical mesoporous films used in this work obtained by water adsorption–desorption isotherms at 298 K (see upper insets). TEM images of the mesoporous films tested in this study (see lower inserts).

Table 1 Contact angle measurements and structural data of the mesoporous thin films obtained from ellipsoporosimetry

Film type	Pore size (nm)	Thickness (nm)	Porosity (%)	Contact angle (°)
MSi-9	9.2 ± 0.8	100 ± 1	37 ± 2	28 ± 2
MSi-4	4.1 ± 0.5	150 ± 1	42 ± 2	16 ± 1
NMSi	—	93 ± 1	5 ± 0.5	29 ± 2
MTi-10	10.2 ± 0.9	145 ± 1	37 ± 2	31 ± 2
MTi-6	6.4 ± 0.5	92 ± 1	47 ± 2	15 ± 1
NMTi	—	56 ± 1	<2	40 ± 2

DAPI staining revealed that 3 h after cell seeding the number of adhered cells was significantly higher on the $NMTiO_2$-coated surfaces. In the case of SiO_2 films, a higher number of adhered cells was found on MSi-4 (74 cells per cm^2) and NMSi (67 cells per cm^2) followed by MSi-9 (18 cells per cm^2). Among the TiO_2 films, a higher number of cells were observed on NMTi (131 cells per cm^2), followed by the mesoporous films MTi-10 and MTi-6, with 84 and 81 cells per cm^2, respectively. In addition, this trend is maintained for t = 6 h. These observations suggest that in the case of titanium dioxide, the hydrophilic or hydrophobic character of the surface, rather than the pore texture, is the key parameter influencing cell adhesion at short times. This is coincident with previous reports on self-assembled monolayers, in which hydrophobic CH_3-terminated surfaces promote cell adhesion and proliferation, while PEG-modified surfaces lead to lower cell numbers.[18]

At the same time, MSi-4 and MSi-9 presented a higher number of adhered cells than NMSi, although the differences are not statistically significant. These results do not allow us to suggest that, in the case of Si films, mesoporous surfaces with lower pore diameters are more suitable for cell adhesion. In addition, the influence of hydrophilic or hydrophobic properties of the Si films is not as clear as it is in the case of Ti films (NMSi = 29°, MSi-9 nm = 28° and MSi-4 nm = 16°). In the case of the Si films, MSi-4 displays the lowest contact angle (16°) and the highest number of adhered cells. These differences within the Si films can be explained by the effect of two factors: on the one hand silica films are prone to dissolve in culture medium and on the other hand the adsorption capacity of silica materials may favour protein adsorption to the films, thus the cells are in contact with the adsorbed protein layer instead of the bare surface. Indeed, the protein layer is the intermediate that interacts with integrins and other cell membrane receptors that mediate cell adhesion.[19] However, surface hydrophobicity has been widely identified as a key factor in determining protein and cell surface interactions, the water contact angle alone does not enable us to fully describe these interactions because different surfaces may have the same contact angle.

A different situation appears after 24 h; there is a reduction in the adhered cells[20] and mesoporosity seems to be the main parameter affecting cell adhesion and proliferation (Fig. 2A). A significantly different behaviour from the one observed at short times is noticed, in which the lower the porosity, the

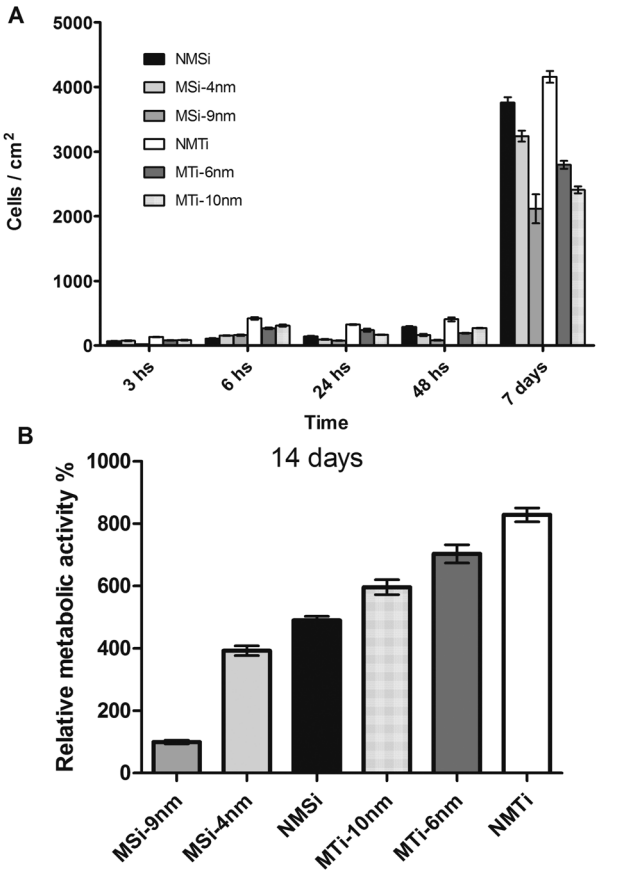

Fig. 2 (A) Number of adhered cells per cm^2 determined by DAPI staining (for statistical analysis see ESI†), (B) MTT results. Relative metabolic activity after 14 days. MSi-9 nm was assigned as 100%. All samples are statistically different ($p < 0.05$).

higher the number of detected cells. This new trend is reproducible and remains even after 14 days incubation. Fig. 2B shows in detail that the degree of cell proliferation in the long term can be determined by the coating chemical nature and porosity for both Si and Ti films. If the pore size is large, attachment and proliferation of the cells is reduced. This trend was also observed in templated Ti films calcined at different temperatures, where low temperatures induce pores of 4 nm, which have been reported to be more suitable for cell adhesion. In contrast, calcination at high temperatures induces a grid-like structure with pores of 12 nm, which promotes less well-spread cells with higher circularities.[21] Moreover, it was also reported that cells preferentially adhere to mesoporous silicon substrates with an average pore size of 5 nm over substrates with a pore size of 20 nm.[22] In addition, the nature of the inorganic framework is also a central factor, and cell proliferation is more extended onto titania films. As observed in Fig. 2B, these two factors can be advantageously used in order to regulate cell proliferation onto a substrate with a given composition and pore structure. The growth rates between 6 h and 7 days were NMSi: 35, MSi-4 nm: 31, MSi-9 nm: 13, NMTi: 10.5, MTi-6 nm: 10 and MTi-10 nm: 8. Thus, Ti substrates favour the adhesion of a higher number of cells but promote a lower cell proliferation rate than Si substrates do. This effect of Si substrates could be explained in terms of Si dissolution and its well known stimulating effect over osteoblast like cells.

In conclusion, for the first time to our knowledge, a simple method is introduced that allows cell manipulation on surfaces by rationally controlling the surface nanoporosity. This designed strategy was based on the tailored preparation of mesoporous coatings by a combination of sol–gel and supramolecular templating. The cellular response was dependent on both physicochemical and nano-topographical stimuli. Particularly, it was shown that in the short term (*i.e.* 3–6 hours), the initial events at the surface are governed by the hydrophilic/hydrophobic properties of the surface, which creates an interface to which the cell responds with different degrees of adhesion. Moreover, in the long term (days), the nanotopography and chemistry of the surface determine how cells will attach and proliferate. In this sense, it was demonstrated that it is possible to tune cell adhesion and proliferation by controlled nanoporosity introduced during film formation. It is important to emphasize the simplicity of the procedure used to prepare these nanostructured surfaces that avoids the use of chemical functionalization.

It is worth mentioning that these results further confirm that osteoblasts are sensitive to subtle differences in surface roughness and surface chemistry on the nanometric level. Especially, we report the possibilityof gradually regulating the proliferation of the cells over various surfaces. Finally, these results will contribute to optimizing the surface structure for site-specific tissue engineering applications and a straightforward application of this coating to the improved integration of prosthesis and implants can be anticipated.

Acknowledgements

The authors acknowledge the support of grants from the University of Buenos Aires UBACYT 20020110100081, ANPCyT (PICT 2008-1848, PICT 2010-0026 and PAE-37063-PME-2006-00038), CONICET (PIP 00186) and LNLS (beamline D02A-SAXS2). MFD, MCDM, MGB and GJAASI are CONICET researchers.

Notes and references

1 M. Schernthaner, B. Reisinger, H. Wolinski, S. D. Kohlwein, A. Trantina-Yates, M. Fahrner, C. Romanin, H. Itani, D. Stifter, G. Leitinger, K. Groschner and J. Heitz, *Acta Biomater.*, 2012, **8**, 2953.

2 B. K. K. Teo, K. J. Goh, Z. J. Ng, S. Koo and E. K. F. Yim, *Acta Biomater.*, 2012, **8**, 2941.

3 A. M. C. Barradas, K. Lachmann, G. Hlawacek, C. Frielink, R. Truckenmoller, O. C. Boerman, R. van Gastel, H. Garritsen, M. Thomas, L. Moroni, C. van Blitterswijk and J. de Boer, *Acta Biomater.*, 2012, **8**, 2969.

4 (*a*) S. Quignard, G. J. Copello, C. Aimé, I. Bataille, C. Hélary, M. F. Desimone and T. Coradin, *Adv. Eng. Mater.*, 2012, **14**, B51; (*b*) M. F. Desimone, C. Hélary, G. Mosser, M.-M. Giraud-Guille, J. Livage and T. Coradin, *J. Mater. Chem.*, 2010, **20**, 666.
5 I. Wall, N. Donos, K. Carlqvist, F. Jones and P. Brett, *Bone*, 2009, **45**, 17.
6 M. F. Desimone, C. Hélary, S. Quignard, I. B. Rietveld, I. Bataille, G. J. Copello, G. Mosser, M. M. Giraud-Guille, J. Livage, A. Meddahi-Pellé and T. Coradin, *ACS Appl. Mater. Interfaces*, 2011, **3**, 3831.
7 C. D. W. Wilkinson, M. Riehle, M. Wood, J. Gallagher and A. S. G. Curtis, *Mater. Sci. Eng., C*, 2002, **19**, 263.
8 J. J. Norman and T. A. Desai, *Ann. Biomed. Eng.*, 2006, **34**, 89.
9 F. Gentile, L. Tirinato, E. Battista, F. Causa, C. Liberale, E. M. di Fabrizio and P. Decuzzi, *Biomaterials*, 2010, **31**, 7205.
10 G. J. A. A. Soler-Illia, P. C. Angelomé, M. C. Fuertes, A. Calvo, A. Wolosiuk, A. Zelcer, M. G. Bellino and E. D. Martínez, *J. Sol-Gel Sci. Technol.*, 2011, **57**, 299.
11 G. J. A. A. Soler-Illia, P. C. Angelomé, M. C. Fuertes, D. Grosso and C. Boissiere, *Nanoscale*, 2012, **4**, 2549.
12 C. Sanchez, C. Boissière, D. Grosso, C. Laberty and L. Nicole, *Chem. Mater.*, 2008, **20**, 682.
13 F. Cagnol, D. Grosso, G. J. D. A. A. Soler-Illia, E. L. Crepaldi, F. Babonneau, H. Amenitsch and C. Sanchez, *J. Mater. Chem.*, 2003, **13**, 61.
14 E. L. Crepaldi, G. J. D. A. A. Soler-Illia, D. Grosso, F. Cagnol, F. Ribot and C. Sanchez, *J. Am. Chem. Soc.*, 2003, **125**, 9770.
15 C. Boissiere, D. Grosso, S. Lepoutre, L. Nicole, A. B. Bruneau and C. Sanchez, *Langmuir*, 2005, **21**, 12362.
16 T. Mosmann, *J. Immunol. Methods*, 1983, **65**, 55.
17 M. Järn, F. J. Brieler, M. Kuemmel, D. Grosso and M. Lindén, *Chem. Mater.*, 2008, **20**, 1476.
18 H. Schweikl, R. Müller, C. Englert, K. A. Hiller, R. Kujat, M. Nerlich and G. Schmalz, *J. Mater. Sci.: Mater. Med.*, 2007, **18**, 1895.
19 E. Ruoslahti and M. D. Pierschbacher, *Science*, 1987, **238**, 491.
20 M. F. Desimone, M. C. De Marzi, G. S. Alvarez, I. Mathov, L. E. Diaz and E. L. Malchiodi, *J. Mater. Chem.*, 2011, **21**, 13865–13872.
21 J. D. Bass, E. Belamie, D. Grosso, C. Boissiere, T. Coradin and C. Sanchez, *J. Biomed. Mater. Res., Part A*, 2010, **93**, 96.
22 F. Gentile, R. La Rocca, G. Marinaro, A. Nicastri, A. Toma, F. Paonessa, G. Cojoc, C. Liberale, F. Benfenati, E. di Fabrizio and P. Decuzzi, *ACS Appl. Mater. Interfaces*, 2012, **4**, 2903.